Synthesis, Crystal Structure and Magnetic Properties of the Alternating Chain $[VO(H_2O)_5][Cu_2(bipym)_2(H_2O)(SO_4)_3]\cdot 7H_2O$ (bipym = 2,2'-bipyrimidine)†

Giovanni De Munno,[a] **Carla Bazzicalupi,**[b] **Juan Faus,**[c] **Francesc Lloret**[c] **and Miguel Julve** *[,c]
[a] *Dipartimento di Chimica, Università degli Studi della Calabria, 87030 Arcavacata di Rende, Cosenza, Italy*
[b] *Dipartimento di Chimica, Università degli Studi di Firenze, Via Maragliano 75/77, 50144 Firenze, Italy*
[c] *Departament de Química Inorgànica, Facultat de Química de la Universitat de València, Dr. Moliner 50, 46100 Burjassot, València, Spain*

The new compound $[VO(H_2O)_5][Cu_2(bipym)_2(H_2O)(SO_4)_3]\cdot 7H_2O$ **1** (bipym = 2,2'-bipyrimidine) has been synthesised and its crystal structure determined by single-crystal X-ray diffraction [monoclinic, space group $P2_1/c$, $a = 9.944(3)$, $b = 13.928(6)$, $c = 26.275(6)$ Å, $\beta = 99.59(2)°$ and $Z = 4$]. Its structure consists of anionic alternating zigzag chains of bipym-bridged copper(II) ions with aqua and sulfato ligands. The electroneutrality is achieved by pentaaquaoxovanadium(IV) cations. The co-ordination geometry around the copper(II) ions can be described as distorted CuN_4O_2 octahedra: that around Cu(1) comprises three nitrogens from bipym and an oxygen from sulfate in the basal positions and a nitrogen from bipym and an oxygen of another sulfate group in the axial sites; three nitrogens from bipym and an oxygen from sulfate occupy the equatorial positions around Cu(2), whereas a nitrogen from bipym and an oxygen from water fill the axial sites. The bipyrimidine group joins two adjacent copper atoms acting in a bis(chelating) fashion. The vanadium atom in the pentaaquavanadyl cation is approximately at the centre of an octahedron defined by five oxygens from water molecules and an oxo group. The V^{IV}–O (oxo) bond distance [1.577(5) Å] is shorter than that of V^{IV}–O(water) (average 2.025 Å). The intrachain copper–copper separations are 5.505(2) and 5.675(2) Å. Variable-temperature (4.2–300 K) magnetic susceptibility data were fitted by the alternating-chain spin-exchange model [$\hat{H} = -J\Sigma(\hat{S}_{2i}\cdot\hat{S}_{2i-1} + \alpha\hat{S}_{2i}\cdot\hat{S}_{2i+1})$, α = alternation parameter] and to the usual Bleaney–Bowers expression for a copper(II) pair with the inclusion in both cases of the Curie law for an isolated $S = \frac{1}{2}$ species in order to account for the presence of the vanadyl cation. The values of the exchange coupling are discussed in the light of the structural data and compared to those reported for other bipym-bridged copper(II) complexes.

In the last fifteen years, many magneto-structural studies dealing with one-dimensional systems have been made,[1–5] with particular attention being paid to homometallic alternating chains. This kind of chain has in common either the alternating bridging ligand or the alternating spacing. Although the most appropriate strategy in designing alternating chains would be based on the use of two different potentially bridging ligands,[6–13] the chemistry literature is very rich with examples of the first group which concerns mainly the copper(II) halide oligomers[14–17] where the same atom bridges the metal ions in two different and regularly alternated fashions.

In the course of our research on the structural characterization and magnetic properties of 2,2'-bipyrimidine (bipym)-bridged first-row transition-metal ions[13,18–21] we obtained a polynuclear compound of formula $[VO(H_2O)_5][Cu_2(bipym)_2(H_2O)(SO_4)_3]\cdot 7H_2O$ **1** in which the copper(II) ions are bridged by two different bis(chelating) bipym ligands in a regular alternating fashion. We report here the preparation and crystal structure of this compound together with a description of its magnetic properties as a function of temperature.

Experimental

Materials.—2,2'-Bipyrimidine (Lancaster Synthesis) and pentahydrated forms of vanadyl(IV) and copper(II) sulfates (Merck) were used as received. Elemental analyses (C, H, N) were conducted by the Microanalytical Service of the Universidad Autónoma de Madrid (Spain).

Preparation of $[VO(H_2O)_5][Cu_2(bipym)_2(H_2O)(SO_4)_3]\cdot 7H_2O$ **1**.—This compound was obtained as blue-greenish prismatic crystals by slow evaporation at room temperature of aqueous solutions containing stoichiometric amounts of the metal sulfates and bipym. Partial oxidation of V^{IV} to V^{V} occurs if the solutions are heated. The crystals were filtered off, washed with small amounts of cold water and ethanol and dried over filter-paper. They are stable in the open air. Apart from bands characteristic of unidentate sulfate [1104vs (ν_3), 1040s (ν_3), 620s and 605 (sh) cm^{-1} (ν_4)] the IR spectrum exhibits a broad and strong absorption between 3600 and 3100 cm^{-1} (antisymmetric and symmetric OH stretching) with a medium-intensity peak at 1640 cm^{-1} (HOH bending) showing the presence of both co-ordinated and lattice water molecules,[22] ν(V=O) at 980m cm^{-1} and finally a very asymmetric triplet at 1585s, 1575vw and 1560vw cm^{-1} (ring stretching modes of bipym) which is consistent with the occurrence of bis(chelating) bipym[18a] (Found: C, 18.50; H, 3.85; N, 10.75. Calc. for $C_{16}H_{38}Cu_2N_8O_{26}S_3V$ **1**: C, 18.60; H, 3.70; N, 10.85%).

Physical Techniques.—Infrared spectra were recorded on a Perkin-Elmer 1750 FTIR spectrophotometer as KBr pellets in the 4000–300 cm^{-1} region, X-band ESR spectra using a Brüker ER-200D spectrometer equipped with a helium continuous-

---

† *Supplementary data available:* see Instructions for Authors, *J. Chem. Soc., Dalton Trans.*, 1994, Issue 1, pp. xxiii–xxviii

Non-SI units employed: emu = SI × $10^6/4\pi$, G = 10^{-4} T.

Table 1 Crystallographic data for $[VO(H_2O)_5][Cu_2(bipym)_2(H_2O)(SO_4)_3]\cdot 7H_2O$ **1**

Formula	$C_{16}H_{38}Cu_2N_8O_{26}S_3V$
M	1032.7
Crystal system	Monoclinic
Space group	$P2_1/c$
a/Å	9.944(3)
b/Å	13.928(6)
c/Å	26.275(6)
β/°	99.59(2)
U/Å^3	3588(2)
Z	4
D_c/kg m^{-3}	1.912
$F(000)$	2108
Crystal size/mm	0.55 × 0.30 × 0.25
μ(Mo-Kα)/cm^{-1}	17.1
Scan method	ω–2θ
2θ range/°	3–50
No. of refined parameters, N_p	583
$R\{= [\Sigma(\lvert\lvert F_o\rvert - \lvert F_c\rvert\rvert)/\Sigma\lvert F_o\rvert]\}$	0.0451
$R'\{=[\Sigma(\lvert\lvert F_o\rvert - F_c\rvert)^2/\Sigma w\lvert F_o\rvert^2]^{\frac{1}{2}}\}$	0.0447
S*	1.56

* Goodness of fit = $[\Sigma w(\lvert\lvert F_o\rvert - \lvert F_c\rvert\rvert)^2/(N_o - N_p)]^{\frac{1}{2}}$.

flow cryostat. Variable-temperature magnetic susceptibility measurements were carried out in the range 4.2–300 K with a fully automatized AZTEC DSM8 pendulum-type susceptometer equipped with a TBT continuous-flow cryostat and a Brüker BE15 electromagnet, operating at 1.8 T. The apparatus was calibrated with $Hg[Co(NCS)_4]$. Corrections for diamagnetism were estimated from Pascal's constants[23] as -521×10^{-6} emu mol^{-1}.

Crystallography.—Diffraction data for complex **1** were collected at 298 K with a CAD-4 Enraf–Nonius automatic four-circle diffractometer using graphite-monochromated Mo-Kα radiation (λ = 0.710 69 Å). Table 1 summarizes the crystallographic and selected experimental data. The unit-cell parameters were determined from least-squares refinement of the setting angles of 25 reflections in the range 2θ 15–30°. Three standard reflections were monitored after every 100 during the data collection and no significant decay was observed. A total of 6654 reflections were collected by the variable-speed ω–2θ scan method in the range 2θ 3–50° with index ranges $-11 \leqslant h \leqslant 11$, $0 \leqslant k \leqslant 16$, $0 \leqslant l \leqslant 31$; 5680 of them were unique, and of these 4323 were assumed as observed $[I > 3\sigma(I)]$ and used for the refinement. The intensities were corrected for Lorentz and polarization effects. An absorption correction was also applied using the method of Stuart and Walker.[24] The maximum and minimum transmission factors were 0.63 and 0.50.

The structure was solved by standard Patterson methods and subsequently completed by Fourier recycling. All non-hydrogen atoms were refined anisotropically. The hydrogen atoms of the water molecules were located on a ΔF map and refined with constraints. The hydrogen atoms of bipym were set in calculated positions and refined as riding atoms. A common fixed isotropic thermal parameter was assigned to all hydrogen atoms (U_{iso} = 50 Å^2). The final full-matrix least-squares refinement, minimizing the function $\Sigma w(\lvert\lvert F_o\rvert - \lvert F_c\rvert\rvert)^2$ with $w^{-1} = \sigma^2(F_o) + 0.0004(F_o)^2$ [with $\sigma^2(F_o)$ from counting statistics], converged at R and R' indices of 0.0451 and 0.0447. The number of reflections/number of variable parameters was 7.4. In the final difference map the residual maxima and minima were 0.55 and -0.73 e Å^{-3}. The largest and mean Δ/σ were 0.530 and 0.014. Solutions and refinements were performed with the SHELXTL PLUS system.[25] The final geometrical calculations were carried out with the PARST[26] program. The graphical manipulations were performed using the XP utility of the SHELXTL PLUS system. Final atomic coordinates for non-hydrogen atoms and selected bond lengths and angles are given in Tables 2 and 3.

Additional material available from the Cambridge Crystallographic Data Centre comprises H-atom coordinates, thermal parameters and remaining bond lengths and angles.

Results and Discussion

Description of the Structure.—The structure of complex **1** is made up of anionic zigzag chains of bipyrimidine-bridged copper(II) ions of formula $[Cu_2(bipym)_2(H_2O)(SO_4)_3]^{2-}$, pentaaquaoxovanadium(IV) cations and crystallization water molecules. A view of the asymmetric dinuclear unit within the chain and of a symmetry-related fragment with the atom-labelling scheme is depicted in Fig. 1, whereas the corresponding perspective view of the co-ordination geometry about the vanadium atom in $[VO(H_2O)_5]^{2+}$ is shown in Fig. 2. The anionic chains grow along the a axis, the vanadyl cations and the crystallization water molecules being located between them. An extensive network of hydrogen bonds links oxygen atoms from co-ordinated sulfate groups and co-ordinated and unco-ordinated water molecules as shown in Table 4.

A regular alternation of two non-equivalent copper atoms [Cu(1) and Cu(2)] occurs in the chain. Both exhibit a distorted *cis*-octahedral CuN_4O_2 environment. This chromophore involves a *trans* elongation. The four nitrogen atoms of a bridging bipym ligand [N(1), N(2), N(3) and N(4)] occupy equatorial positions of two octahedra [N(1) and N(3) at Cu(1) and N(2) and N(4) at Cu(2)], the two remaining equatorial sites being filled by oxygen atoms from sulfate groups [O(2) at Cu(1) and O(9) at Cu(2)] and nitrogen atoms from a second and a third bipym group [N(7) at Cu(1) and N(5a) at Cu(2)]. Six-co-ordination is achieved by means of the remaining nitrogen atoms from the second and third bipym molecules [N(6) and N(8a) for Cu(1) and Cu(2), respectively] and two oxygen atoms, one from a sulfate anion [O(5) at Cu(1)] and the other from a water molecule [O(13) at Cu(2)]. The three equatorial Cu–N(bipym) bond lengths around both copper atoms occur in two sets: two are very similar and somewhat shorter [2.025(5) and 2.015(5) Å for Cu(1)–N(3) and Cu(1)–N(7), and 2.009(5) and 1.994(5) Å for Cu(2)–N(2) and Cu(2)–N(5a)] than the other [2.094(4) and 2.107(5) Å for Cu(1)–N(1) and Cu(2)–N(4), respectively]. Anyway, they are all significantly shorter than the axial ones [2.304(5) and 2.286(5) Å for Cu(1)–N(6) and Cu(2)–N(8a), respectively]. There is a significant shortening of the equatorial Cu–O(sulfate) bond distances [2.001(4) and 2.015(4) Å for Cu(1)–O(2) and Cu(2)–O(9), respectively] with respect to the parent axial one [2.270(4) Å for Cu(1)–O(5)]. The largest deviations from the mean equatorial planes N(1)N(3)N(7)O(2) and N(2)N(4)N(5a)O(9) are 0.107(5) Å for N(3) and 0.086(5) Å for N(2). Atoms Cu(1) and Cu(2) are 0.018(1) and 0.022(1) Å out of these planes, respectively. There is a large deviation from the idealized orthogonal geometry at the metal atom in the five-membered chelate rings [80.7(2), 80.9(2), 77.4(2) and 78.2(2)° for N(1)–Cu(1)–N(3), N(2)–Cu(2)–N(4), N(6)–Cu(1)–N(7) and N(5a)–Cu(2)–N(8a)] as expected due to the geometric constraints of chelating bipym. The decrease observed in the magnitude of the bite angle in this series is due to the lengthening of the Cu–N(bipym) axial bonds with respect to the equatorial ones. These values for the bite angle are in agreement with those reported for other bipym-bridged copper(II) complexes.[13,18]

Two different bis(chelating) bipym ligands alternate regularly in the chain leading to two intrachain metal–metal separations, 5.505(2) and 5.675(2) Å for Cu(1)$\cdots$Cu(2) and Cu(1)$\cdots$Cu(2b), respectively. This trend of values follows that of the Cu–N(bridging bipym) bond lengths. Indeed, the occurrence of two bipym bridges in the present compound is the main difference from the parent one-dimensional complex $[Cu(bipym)(H_2O)_2][ClO_4]_2\cdot H_2O$[18c,27] in which the copper atoms

Table 2 Final atomic coordinates for complex 1 with estimated standard deviations (e.s.d.s) in parentheses

Atom	*X/a*	*Y/b*	*Z/c*	Atom	*X/a*	*Y/b*	*Z/c*
Cu(1)	0.5658(1)	0.3591(1)	0.3361(1)	N(4)	0.9309(5)	0.2609(3)	0.2989(2)
Cu(2)	1.0635(1)	0.1783(1)	0.3527(1)	N(5)	0.2117(4)	0.1756(3)	0.3102(2)
S(1)	0.3408(1)	0.4268(1)	0.2422(1)	C(9)	0.2160(6)	0.1158(4)	0.2708(2)
O(1)	0.3040(4)	0.5208(3)	0.2170(2)	C(10)	0.3281(6)	0.1121(5)	0.2465(2)
O(2)	0.4642(4)	0.4451(3)	0.2819(2)	C(11)	0.4371(6)	0.1693(5)	0.2657(3)
O(3)	0.2301(4)	0.3916(3)	0.2669(2)	N(6)	0.4328(5)	0.2295(3)	0.3052(2)
O(4)	0.3744(5)	0.3571(3)	0.2044(2)	C(12)	0.3183(5)	0.2316(4)	0.3249(2)
S(2)	0.7954(1)	0.5030(1)	0.4063(1)	C(13)	0.3108(5)	0.3031(4)	0.3664(2)
O(5)	0.6619(4)	0.4975(3)	0.3705(2)	N(7)	0.4177(4)	0.3612(3)	0.3800(2)
O(6)	0.8347(4)	0.6051(3)	0.4114(2)	C(14)	0.4114(6)	0.4226(4)	0.4190(2)
O(7)	0.7764(5)	0.4650(3)	0.4560(2)	C(15)	0.2993(6)	0.4260(5)	0.4433(3)
O(8)	0.8964(4)	0.4486(3)	0.3844(2)	C(16)	0.1913(6)	0.3669(5)	0.4248(2)
S(3)	1.2973(2)	0.0519(1)	0.4185(1)	N(8)	0.1970(5)	0.3042(3)	0.3863(2)
O(9)	1.1594(4)	0.0957(3)	0.4105(2)	O(13)	0.9755(4)	0.0384(3)	0.3202(2)
O(10)	1.3070(4)	−0.0109(3)	0.4637(2)	V	0.5238(1)	0.2295(1)	0.0695(1)
O(11)	1.3168(5)	−0.0029(3)	0.3733(2)	O(26)	0.5355(4)	0.1475(3)	0.0291(2)
O(12)	1.3998(5)	0.1276(4)	0.4270(2)	O(14)	0.7322(4)	0.2392(3)	0.0907(2)
N(1)	0.6989(4)	0.2763(3)	0.3888(2)	O(15)	0.5247(4)	0.3430(3)	0.0225(2)
C(1)	0.6941(6)	0.2492(4)	0.4369(2)	O(16)	0.3194(4)	0.2432(3)	0.0579(2)
C(2)	0.7967(6)	0.1959(4)	0.4649(2)	O(17)	0.5337(5)	0.3406(3)	0.1283(2)
C(3)	0.9067(6)	0.1713(4)	0.4423(2)	O(18)	0.5111(5)	0.1473(3)	0.1320(2)
N(2)	0.9133(4)	0.2002(3)	0.3939(2)	O(19)	0.1358(5)	0.2502(4)	0.1625(2)
C(4)	0.8085(5)	0.2505(4)	0.3696(2)	O(20)	0.7298(5)	0.1396(3)	0.2015(2)
C(5)	0.8188(5)	0.2837(4)	0.3173(2)	O(21)	0.3497(5)	0.5468(4)	0.1169(2)
N(3)	0.7140(5)	0.3352(3)	0.2933(2)	O(22)	0.8912(5)	0.1362(4)	0.0437(2)
C(6)	0.7249(6)	0.3685(4)	0.2462(2)	O(23)	0.2041(6)	0.4181(3)	0.0475(2)
C(7)	0.8391(6)	0.3506(5)	0.2246(2)	O(24)	−0.0409(6)	0.3744(4)	0.1090(2)
C(8)	0.9414(6)	0.2949(5)	0.2519(2)	O(25)	0.9496(6)	0.0226(4)	0.1877(2)

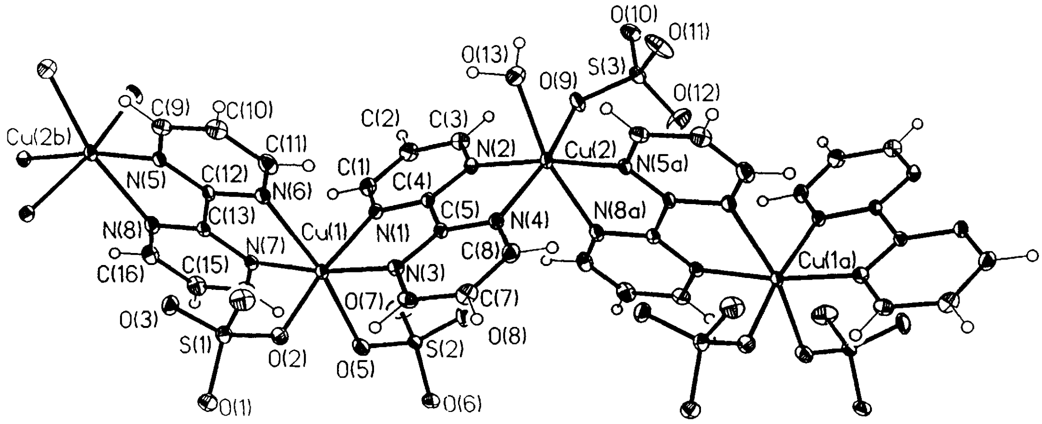

Fig. 1 Perspective view of the anionic chain $[Cu_2(bipym)_2(H_2O)(SO_4)_3]^{2-}$ showing the atom labelling. Thermal ellipsoids are drawn at the 30% probability level

are equivalent. The pyrimidyl rings of both bipym bridging ligands are planar as expected [the larger deviations from the corresponding mean planes are 0.011(6) Å at C(5) in C(5)-N(3)C(6)C(7)C(8)N(4) and 0.025(6) Å at C(12) in N(5)C(9)-C(10)C(11)N(6)C(12)] and each of the bipym ligands as a whole shows small deviations from planarity [dihedral angles between the mean planes N(1)C(1)C(2)C(3)N(2)C(4) and C(5)N(3)C(6)-C(7)C(8)N(4) and N(5)C(9)C(10)C(11)N(6)C(12) and C(13)-N(7)C(14)C(15)C(16)N(8) are 4.3(2) and 1.8(1)°, respectively]. No significant differences are observed in the carbon–carbon and -nitrogen intraring bonds of the two bridging bipym groups (average values 1.375 and 1.334 Å, respectively) and their values compare well with that of both free[28] and co-ordinated bipym.[13,18,27,29] The carbon–carbon interring bond length [1.468(8) and 1.489(8) Å for C(4)–C(5) and C(12)–C(13)] is significantly shortened with respect to that of a single carbon–carbon bond. Atoms Cu(1) and Cu(2) are only 0.014(1) and 0.027(1) Å below and above the N(1)C(1)C(2)C(3)N(2)C(4)-C(5)N(3)C(6)C(7)C(8)N(4) mean plane. However, they are significantly displaced [0.313(1) Å for Cu(1) towards N(1) and 0.273(1) Å for Cu(2b) towards N(4b)] from the N(5)-C(9)C(10)C(11)N(6)C(12)C(13)N(7)C(14)C(15)C(16)N(8) bipym plane. The adjacent bipym ligands within the chain form a dihedral angle of 102.1(1)°. The intrachain bipym–bipym distance between bipym molecules which only form equatorial bonds with copper atoms is larger [3.896(6) Å] than that observed for the other type of bipym [2.803(6) Å].

The co-ordinated sulfate groups have their expected tetrahedral geometry. The S–O(co-ordinated to copper) bond distances [1.495(4), 1.496(4) and 1.483(4) Å for S(1)–O(2), S(2)–O(5) and S(3)–O(9), respectively] are somewhat larger than the remaining sulfur–oxygen bonds [averages 1.47, 1.46 and 1.46 Å for S(1), S(2) and S(3)]. The average intraion bond angle is 109.4(2), 109.5(3) and 109.5(3)° for S(1), S(2) and S(3), respectively.

The vanadium atom of the $[VO(H_2O)_5]^{2+}$ unit in complex **1** is approximately at the centre of a distorted octahedron comprising five water molecules and an oxo group. Its geometry is similar to that of the related complexes $[VO(H_2O)_5]SO_4$ **2**[30] and $[VO(H_2O)_5]SO_4{\cdot}H_2O$ **3**.[31] The average value of the four

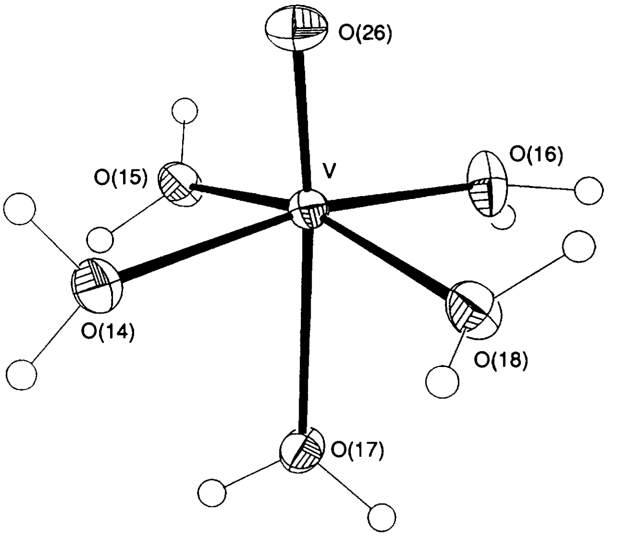

Fig. 2 Perspective drawing of the vanadyl $[VO(H_2O)_5]^{2+}$ cation showing the atom labelling. Thermal ellipsoids are as in Fig. 1

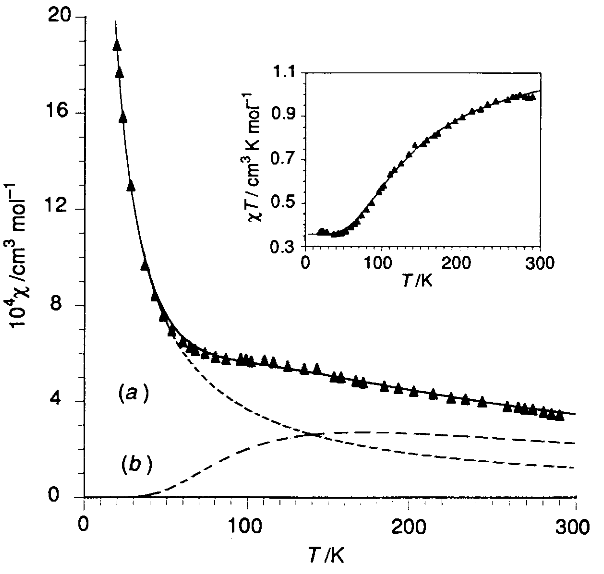

Fig. 3 Thermal dependence of χ_M (▲) ($\chi_M T$ in the insert) for complex **1**; (—) best theoretical fit by using equation (1) (see text). The dashed lines (*a*) and (*b*) correspond to the calculated susceptibilities per one vanadium(IV) and two copper(II) ions, respectively

Table 3 Selected interatomic distances (Å) and bond angles (°) for complex **1** with e.s.d.s in parentheses *

Copper environment			
Cu(1)–O(2)	2.001(4)	Cu(2)–O(9)	2.015(4)
Cu(1)–O(5)	2.270(4)	Cu(2)–N(2)	2.009(5)
Cu(1)–N(1)	2.094(4)	Cu(2)–N(4)	2.107(5)
Cu(1)–N(3)	2.025(5)	Cu(2)–O(13)	2.246(5)
Cu(1)–N(6)	2.304(5)	Cu(2)–N(5a)	1.994(5)
Cu(1)–N(7)	2.015(5)	Cu(2)–N(8a)	2.286(5)
O(2)–Cu(1)–O(5)	84.5(2)	O(9)–Cu(2)–O(13)	84.0(2)
O(2)–Cu(1)–N(1)	171.2(2)	O(9)–Cu(2)–N(2)	89.0(2)
O(2)–Cu(1)–N(3)	91.8(2)	O(9)–Cu(2)–N(4)	169.3(2)
O(2)–Cu(1)–N(6)	91.5(2)	O(9)–Cu(2)–N(5a)	96.3(2)
O(2)–Cu(1)–N(7)	93.9(2)	O(9)–Cu(2)–N(8a)	88.6(2)
O(5)–Cu(1)–N(1)	91.6(2)	O(13)–Cu(2)–N(2)	93.4(2)
O(5)–Cu(1)–N(3)	93.6(2)	O(13)–Cu(2)–N(4)	93.3(2)
O(5)–Cu(1)–N(6)	169.8(2)	O(13)–Cu(2)–N(5a)	92.8(2)
O(5)–Cu(1)–N(7)	93.5(2)	O(13)–Cu(2)–N(8a)	167.6(2)
N(1)–Cu(1)–N(3)	80.7(2)	N(2)–Cu(2)–N(4)	80.9(2)
N(1)–Cu(1)–N(6)	93.7(2)	N(2)–Cu(2)–N(5a)	172.3(2)
N(1)–Cu(1)–N(7)	94.1(2)	N(2)–Cu(2)–N(8a)	96.4(2)
N(3)–Cu(1)–N(6)	95.9(2)	N(4)–Cu(2)–N(5a)	94.1(2)
N(3)–Cu(1)–N(7)	171.3(2)	N(4)–Cu(2)–N(8a)	95.7(2)
N(6)–Cu(1)–N(7)	77.4(2)	N(5a)–Cu(2)–N(8a)	78.2(2)
Vanadyl environment			
V–O(14)	2.059(4)	V–O(15)	2.006(5)
V–O(16)	2.013(4)	V–O(17)	2.176(5)
V–O(18)	2.022(5)	V–O(26)	1.577(5)
O(14)–V–O(15)	90.4(2)	O(14)–V–O(16)	168.5(2)
O(14)–V–O(17)	80.6(2)	O(14)–V–O(18)	90.8(2)
O(14)–V–O(26)	92.6(2)	O(15)–V–O(16)	86.5(2)
O(15)–V–O(17)	82.7(2)	O(15)–V–O(18)	162.3(2)
O(15)–V–O(26)	98.5(2)	O(16)–V–O(17)	88.0(2)
O(16)–V–O(18)	88.8(2)	O(16)–V–O(26)	98.8(2)
O(17)–V–O(18)	80.1(2)	O(17)–V–O(26)	173.2(2)
O(18)–V–O(26)	99.0(2)		

* Symmetry codes: a, 1 + *x*, *y*, *z*; b, *x* − 1, *y*, *z*.

Table 4 Hydrogen bond distances (Å) and angles (°) for complex **1** with e.s.d.s in parentheses *

A	D	H	A···D	A···H–D
O(22)	O(14)	H(14a)	2.59(1)	176(5)
O(23)	O(16)	H(16b)	2.69(1)	157(4)
O(4)	O(17)	H(17a)	2.76(1)	165(5)
O(20)	O(18)	H(18a)	2.60(1)	163(5)
O(4)	O(19)	H(19a)	2.86(1)	163(4)
O(25)	O(20)	H(20a)	2.80(1)	154(5)
O(1)	O(21)	H(21a)	2.77(1)	169(5)
O(21)	O(23)	H(23b)	2.79(1)	153(4)
O(19)	O(24)	H(24b)	2.69(1)	167(5)
O(6^{I})	O(19)	H(19a)	2.85(1)	164(4)
O(1^{I})	O(20)	H(20b)	2.77(1)	175(5)
O(1^{I})	O(13)	H(13b)	2.80(1)	173(3)
O(5^{I})	O(18)	H(18b)	2.70(1)	171(5)
O(6^{I})	O(16)	H(16a)	2.67(1)	159(6)
O(3^{I})	O(25)	H(25a)	2.94(1)	164(5)
O(24^{II})	O(14)	H(14b)	2.92(1)	150(4)
O(10^{III})	O(23)	H(23a)	2.88(1)	148(4)
O(12^{III})	O(15)	H(15a)	2.64(1)	175(5)
O(7^{IV})	O(22)	H(22b)	2.78(1)	161(5)

* A = acceptor, D = donor. Symmetry codes: I, $1 - x, y - \frac{1}{2}, \frac{1}{2} - z$; II, $1 + x, y, z$; III, $x - 1, \frac{1}{2} - y, z - \frac{1}{2}$; IV, $x, \frac{1}{2} - y, z - \frac{1}{2}$.

equatorial V–O(water) bonds in **1** [2.025(4) Å] is very close to that of **2** [2.024(4) Å] and **3** [2.019(2) Å]. However, the axial V–O bond lengths are somewhat different. In particular, the double vanadium to oxygen bond in **1** [1.577(5) Å] is the shortest in the present series [1.519(5) and 1.586(2) Å in **2** and **3**, respectively], while the axial V–O(water) bond distance [2.176(5) Å] is close to that of **3** [2.160(2) Å] but shorter than that of **2** [2.218(5) Å]. The axial O(17)–V–O(26) bond angle in **1** [173.2(2)°] lies between that of **2** [171.9(2)°] and **3** [175.0(1)°]. The best equatorial plane around V is defined by the O(14), O(15), O(16) and O(18) set of atoms, the largest deviation from this mean plane being 0.060(5) Å at O(16). The vanadium atom is displaced by 0.259(1) Å from this plane toward O(26).

Magnetic Properties.—The magnetic properties of complex **1** in the form of plots of χ_M [the magnetic susceptibility per two copper(II) and one vanadyl cation] and $\chi_M T$ *versus* T are depicted in Fig. 3. The decrease of $\chi_M T$ with T in the temperature range 300–50 K and the plateau of $\chi_M T$ at lower temperatures [0.364 cm^3 K mol^{-1} at $T < 50$ K] can easily be explained in terms of antiferromagnetic coupling between copper(II) ions and the presence of magnetically isolated vanadyl cations.

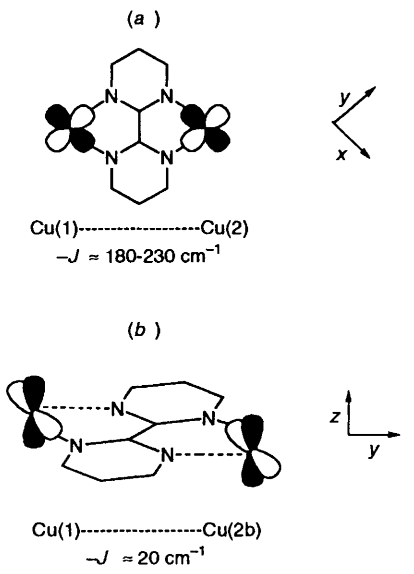

Scheme 1

Based on the structure of complex **1**, two different interpretations of the antiferromagnetic interaction between the copper(II) centres are possible. The first deals with the simpler situation arising from the dimerization within the chain [exchange coupling only through the bipym bridge which forms equatorial bonds with both copper(II) ions], whereas the second corresponds to the alternating-chain description assuming that both types of bipym bridges are able to mediate significant exchange interactions. In fact, the unpaired electron of Cu(1) is described by an essentially $d_{x^2-y^2}$-type magnetic orbital [the *x* and *y* axes are roughly defined by the short Cu–N(bipym) bonds] which is delocalized on the nearest N(1), N(3), N(7) and O(2) neighbours and a similar situation occurs for that of Cu(2), the nearest neighbours being in this case the atoms N(2), N(4), N(5a) and O(9). The strong σ in-plane overlap between these two magnetic orbitals through the N(1)C(4)N(2) and N(3)C(5)N(4) fragments [see Scheme 1(*a*)] would result in important antiferromagnetic coupling.[18a] On the other hand, very weak spin densities on the axial atoms N(6) and N(8a) are expected because of the lengthening of the axial with respect to the equatorial bonds. Consequently, the overlapping of the $d_{x^2-z^2}$-type magnetic orbitals through the N(6)C(12)N(5) and N(7)C(13)N(8) fragments would be very small and the exchange coupling between atoms Cu(1) and Cu(2b) is predicted to be very weak [Scheme 1(*b*)]. Therefore, although the crystal structure of **1** suggests an alternating linear chain, it should be possible to interpret the magnetic data with a simple Bleaney–Bowers equation. Thus, we first treated the experimental susceptibilities with the modified Bleaney–Bowers expression (1) where *J* and g_{Cu} are the singlet–triplet energy gap and the average *g* factor for the copper(II) dimer, and *N*, β and *k* have their usual meanings. The second term is the Curie law accounting for an isolated vanadyl ($S = \frac{1}{2}$) cation. Parameters *J*, g_{Cu} and g_{VO} were determined by least-squares fit minimizing $R = \Sigma[(\chi_M)_{obs} - (\chi_M)_{calc}]^2/\Sigma[(\chi_M)_{obs}]^2$. The values obtained were $J = -190\ \mathrm{cm^{-1}}$, $g_{Cu} = 2.21$, $g_{VO} = 1.97$ and $R = 3 \times 10^{-4}$. The computed curve matches well the experimental one in the whole temperature range investigated. This value for the singlet–triplet energy gap lies within the range of *J* values previously reported for bipym-bridged copper(II) complexes (*J* ranging from −236 to −178 cm^{-1})[18a,b,e] in which the σ in-plane $d_{x^2-y^2}$ exchange pathway is operative.

$$\chi_M = \frac{2N\beta^2 g_{Cu}^2}{kT}[3 + \exp(-J/kT)]^{-1} + \frac{N\beta^2 g_{VO}^2}{4kT} \quad (1)$$

An attempt to fit the magnetic data on the basis of an alternating chain by use of the Hamiltonian $\hat{H} = -J\Sigma(\hat{S}_{2i}\cdot\hat{S}_{2i-1} + \alpha\hat{S}_{2i}\cdot\hat{S}_{2i+1})$ and the development of Hatfield *et al.*[32] led to a practically identical *J* value with an alternation parameter, α, very close to 0.1 and the fit did not improve significantly. The calculated value of α*J* is −19 cm^{-1}, which represents weak coupling, as expected. An identical *J* value was reported for the dinuclear complex $[Cu_2(bipym)_3(H_2O)_4][ClO_4]_4$[18c] the bridge of which reproduces that of the fragment of the present chain. Therefore, the magnetic data do not allow us to decide whether the description of complex **1** as an alternating chain is correct. In cases such as this,[10,11] ESR spectroscopy has proved to be very useful in distinguishing the two interpretations. Unfortunately, we could not take advantage of this complementarity between ESR spectroscopy and magnetic properties. The X-band polycrystalline powder ESR spectrum of **1** at room temperature looks like a quasi-isotropic feature centred at 3225 G without any hyperfine splitting. This is accounted for by the overlapping of copper(II) and oxovanadium(IV) absorptions. At liquid-helium temperatures, there are eight resonance peaks with unequal derivative heights which are due to the hyperfine interaction between the single d electron of the isolated oxovanadium(IV) and the vanadium-51 nuclear spin ($I = \frac{7}{2}$).[33,34] The average *g* value is 1.97 and the separation between the two adjacent features is 208 G. No signal at half field was detected either at room or low temperatures. The vanadyl cation allowed us to obtain single crystals of this novel alternating bipym-bridging copper(II) chain but its presence in the structure precluded a unique interpretation of the observed magnetic properties.

Acknowledgements

Financial support from the Dirección General de Investigación Científica y Técnica (DGICYT) (Spain) through Project PB91-0807-C02-01 and from the Italian Ministero dell'Universitá e della Ricerca Scientifica e Tecnologica is gratefully acknowledged. Thanks are also due to the Servicio de Espectroscopía de la Universitat de València for instrumental facilities.

References

1 W. E. Hatfield, *J. Appl. Phys.*, 1981, **52**, 1985.
2 J. C. Bonner, in *Magneto-Structural Correlations in Exchange Coupled Systems*, eds. R. D. Willett, D. Gatteschi and O. Khan, NATO-ASI Series, Reidel, Dordrecht, 1985, p. 157.
3 R. D. Willett, R. M. Gaura and C. P. Landee, in *Extended Linear Chain Compounds*, ed. J. S. Miller, Plenum, New York, 1983, vol. 3, p. 143.
4 C. P. Landee, in *Organic and Inorganic Low-Dimensional Crystalline Materials*, eds. P. Delhaes and M. Drillon, NATO-ASI Series, Plenum, New York, 1987, p. 75.
5 *Magnetic Molecular Materials*, eds. D. Gatteschi, O. Kahn, J. S. Miller and F. Palacio, NATO-ASI Series, Kluwer, Dordrecht, 1991.
6 M. M. Olmstead, W. K. Musker, L. W. ter Haar and W. E. Hatfield, *J. Am. Chem. Soc.*, 1982, **104**, 6627.
7 B. Chiari, W. E. Hatfield, O. Piovesana, T. Tarantelli, L. W. ter Haar and P. F. Zanazzi, *Inorg. Chem.*, 1983, **22**, 1468.
8 A. Bencini, C. Benelli, D. Gatteschi and C. Zanchini, *J. Am. Chem. Soc.*, 1984, **106**, 5813; C. Benelli, D. Gatteschi, D. W. Carnegie, jun. and R. L. Carlin, *J. Am. Chem. Soc.*, 1985, **107**, 2560.
9 W. E. Hatfield, L. W. ter Haar, M. M. Olmstead and W. K. Musker, *Inorg. Chem.*, 1986, **25**, 558.
10 A. Bencini, C. Benelli, A. C. Fabretti, G. Franchini and D. Gatteschi, *Inorg. Chem.*, 1986, **25**, 1063.
11 F. Lloret, M. Julve, J. Faus, Y. Journaux, M. Philoche-Levisalles and Y. Jeannin, *Inorg. Chem.*, 1989, **28**, 3702.
12 M. L. Kirk, W. E. Hatfield, M. S. Lah, D. Kessissoglou, V. L. Pecoraro, L. W. Morgan and J. D. Petersen, *J. Appl. Phys.*, 1991, **69**, 6013.
13 G. De Munno, M. Julve, F. Lloret, J. Faus, M. Verdaguer and A. Caneschi, *Angew. Chem., Int. Ed. Engl.*, 1993, **32**, 1046.
14 H. J. M. de Groot, L. J. De Jongh, R. D. Willet and J. Reedijk, *J. Appl. Phys.*, 1982, **53**, 8038 and refs. therein; L. J. de Jongh, H. J. M.

de Groot and J. Reedijk, *J. Appl. Phys.*, 1982, **53**, 8027; S. O'Brien, R. M. Gaura, C. P. Landee, B. L. Ramakhrishna and R. D. Willett, *Inorg. Chim. Acta*, 1988, **14**, 83.

15 S. A. Roberts, D. R. Bloomquist, R. D. Willett and H. W. Dodgen, *J. Am. Chem. Soc.*, 1981, **103**, 2603; L. W. ter Haar and W. E. Hatfield, *Inorg. Chem.*, 1985, **24**, 1022.

16 A. Daoud, A. Ben Salah, C. Chappert, J. P. Renard, A. Cheikhrouhou, T. Duc and M. Verdaguer, *Phys. Rev. B*, 1986, **33**, 6253.

17 C. P. Landee, A. Djili, H. Place, B. Scott, R. D. Willett, D. F. Mudgett and M. Newhall, *Inorg. Chem.*, 1988, **27**, 620.

18 (*a*) M. Julve, G. de Munno, G. Bruno and M. Verdaguer, *Inorg. Chem.*, 1988, **27**, 3160; (*b*) M. Julve, M. Verdaguer, G. De Munno, J. A. Real and G. Bruno, *Inorg. Chem.*, 1993, **32**, 795; (*c*) G. De Munno, M. Julve, M. Verdaguer and G. Bruno, *Inorg. Chem.*, 1993, **32**, 2215; (*d*) G. De Munno, M. Julve, F. Nicolò, F. Lloret, J. Faus, R. Ruiz and E. Sinn, *Angew. Chem., Int. Ed. Engl.*, 1993, **32**, 613; (*e*) G. De Munno, J. A. Real, M. Julve and M. Muñoz, *Inorg. Chim. Acta*, 1993, **211**, 227.

19 G. De Munno, M. Julve, F. Lloret and A. Derory, *J. Chem. Soc., Dalton Trans.*, 1993, 1179.

20 E. Andrés, G. De Munno, M. Julve, J. A. Real and F. Lloret, *J. Chem. Soc., Dalton Trans.*, 1993, 2169.

21 G. De Munno, F. Nicolò and M. Julve, *Acta Crystallogr., Sect. C*, 1993, **49**, 1049.

22 K. Nakamoto, *Infrared and Raman Spectra of Inorganic and Coordination Compounds*, 4th edn., Wiley, New York, 1986.

23 A. Earnshaw, *Introduction to Magnetochemistry*, Academic Press, London and New York, 1968.

24 N. Walker and D. D. Stuart, *Acta Crystallogr., Sect. A*, 1983, **39**, 158.

25 SHELXTL PLUS, Version 4.21/V, Siemens Analytical X-ray Instruments Inc., Madison, WI, 1990.

26 M. Nardelli, *Comput. Chem.*, 1983, **7**, 95.

27 L. W. Morgan, K. V. Goodwin, W. T. Pennington and J. D. Petersen, *Inorg. Chem.*, 1992, **31**, 1103.

28 L. Fernholt, C. Rømming and S. Samdal, *Acta Chem. Scand., Ser. A*, 1981, **35**, 707.

29 I. Castro, M. Julve, G. De Munno, G. Bruno, J. A. Real, F. Lloret and J. Faus, *J. Chem. Soc., Dalton Trans.*, 1992, 1739; L. W. Morgan, W. T. Pennington, J. D. Petersen and R. R. Ruminski, *Acta Crystallogr., Sect. C*, 1992, **48**, 163.

30 M. Tachez and F. Théobald, *Acta Crystallogr., Sect. B*, 1980, **36**, 1757.

31 M. Tachez and F. Théobald, *Acta Crystallogr., Sect. B*, 1980, **36**, 249.

32 W. E. Hatfield, W. E. Estes, W. E. Marsh, M. W. Pickens, L. W. ter Haar and R. R. Weller, ref. 3, p. 43.

33 J. Selbin, *Chem. Rev.*, 1965, **65**, 153.

34 A. Bencini and D. Gatteschi, in *Transition Metal Chemistry, A Series of Advances*, eds. G. A. Melson and B. N. Figgis, Marcel Dekker, New York, 1982, vol. 8, pp. 1–175.

Received 9th *December* 1993; *Paper* 3/07295I